

Electronic Supplementary Material (ESI) for Journal of Materials Chemistry B.

This journal is © The Royal Society of Chemistry 2016

Supporting Information

A Novel Fluorescent Chemosensor Based on Tetra-peptide for Measuring Zinc Ions in Aqueous Solutions and Live Cells

Peng Wang,^a Jiang Wu,^{*a} Pingru Su,^a Changfu Shan,^a Panpan Zhou,^a Yushu Ge,^b Dan Liu,^b Weisheng Liu^a and Yu Tang^{*a}

a. Key Laboratory of Nonferrous Metals Chemistry and Resources Utilization of Gansu Province and State Key Laboratory of Applied Organic Chemistry, College of Chemistry and Chemical Engineering, Lanzhou University, Lanzhou, 730000, P. R. China.

b. Collaborative Innovation Center of Chemistry for Life Sciences, School of Life Sciences, University of Sciences and Technology of China, Hefei, 230027, P. R. China.

*Corresponding Author. Tel: 86-931-8912552 Fax: 86-931-8912582. E-mail address: tangyu@lzu.edu.cn.

*Corresponding Author. E-mail address: wujiang@lzu.edu.cn.

Figure Contents

Figure S1. HPLC Chromatogram of HL.

Table S1. HPLC Chromatogram data of HL.

Figure S2. MS (ESI) spectrum of HL.

Figure S3. The stability experiment of the HL in 10 mM HEPES buffer.

Figure S4. Counter anions test of Zn²⁺.

Figure S5. The pH test for HL with Zn²⁺.

Figure S6. UV-vis absorption of HL with Zn²⁺.

Figure S7. The binding constant of L-Zn.

Figure S8. The detection limit for Zn²⁺.

Figure S9. The intensity change of high concentration range.

Figure S10. Fluorescence decay profile of HL, L-Zn.

Figure S11. The full range of mass spectrum of L-Zn.

Figure S12. The mass spectrum analysis of L-Zn.

Figure S13. The theoretical isotope patterns mass spectrum of L-Zn.

Figure S14. Fluorescence response of L-Zn with EDTA.

Table S2. Compared with HL and the atomic absorption spectroscopy.

Figure S15. The optimized configurations for the ligand HL and complex L-Zn.

Figure S16. The HOMO-LUMO energy gaps of HL and L-Zn.

Figure S17. Photo-induced electron transfer (PET) verification.

Figure S18. The stability experiment of the HL in live cells.

Table S3. The concentrations of Zn²⁺ and Cu²⁺ in live cells.

Figure S19. Fluorescence imaging of EDTA in live cells.

Table S4. Comparison of chemosensors for Zn²⁺ assays in the literatures.

HPLC Chromatogram of HL

Sample: HL

Column: 4.6*150 mm, kromasil C18-5

Solvent A: 0.1% Trifluoroacetic acid in 100% Acetonitrile

Solvent B: 0.1% Trifluoroacetic acid in 100% Water

Gradient:	Time	A	B
	0.01 min	5%	95%
	25.0 min	70%	30%

Flow rate: 1.0 ml/min

Wavelength: 214 nm

Volume: 10 μ L

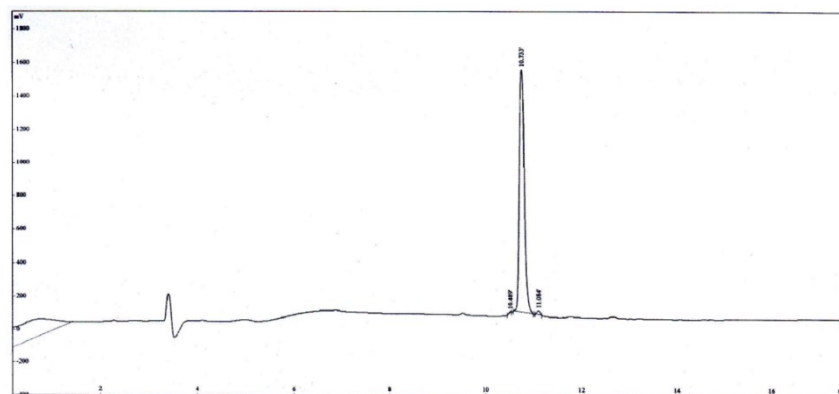


Figure S1. HPLC Chromatogram of HL

Table S1. HPLC Chromatogram data of HL

Rank	Time	Name Conc.	Area
1	10.489	0.3319	35448
2	10.733	98.6011	10530440
3	11.084	1.067	113959
Total		100	10679847

MS Analysis data

Sample: **HL**

Expected MS: 645.2133

Buffer: 0.1% TFA in second distilled water

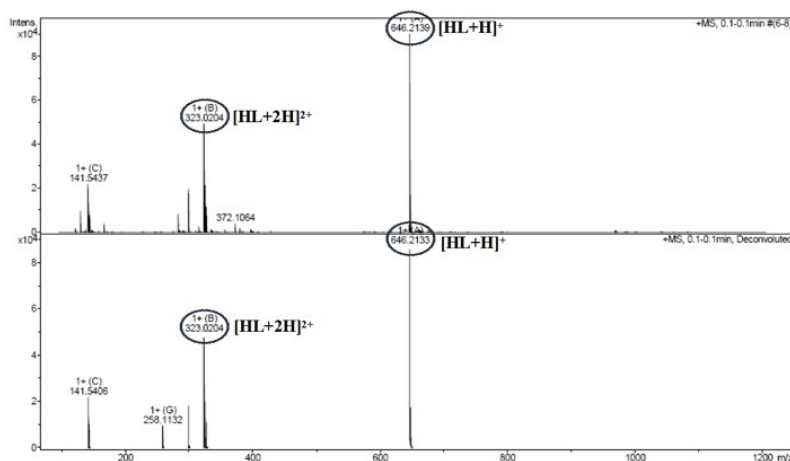


Figure S2. MS (ESI) Spectrum of **HL**.

The stability experiment of the HL in 10 mM HEPES buffer

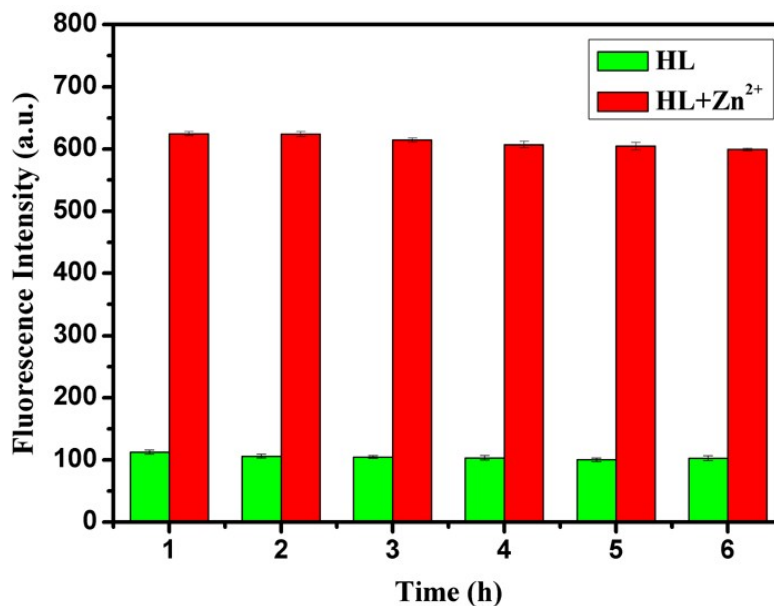


Figure S3. The stability experiment of the **HL** under physiological conditions in 10 mM HEPES buffer at pH 7.4. Error bars represent standard deviations from three repeated experiments.

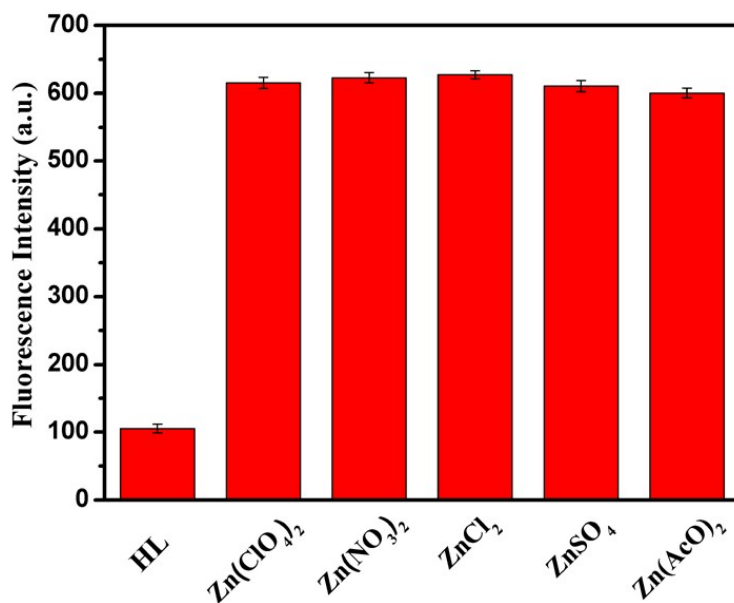
Counter anions test of Zn^{2+} 

Figure S4. Counter anions test of Zn^{2+} with $\text{Zn}(\text{ClO}_4)_2$, $\text{Zn}(\text{NO}_3)_2$, ZnCl_2 , ZnSO_4 and $\text{Zn}(\text{AcO})_2$ (10 mM HEPES buffer, pH 7.4). Excitation wavelength: 330 nm. Error bars represent standard deviations from three repeated experiments.

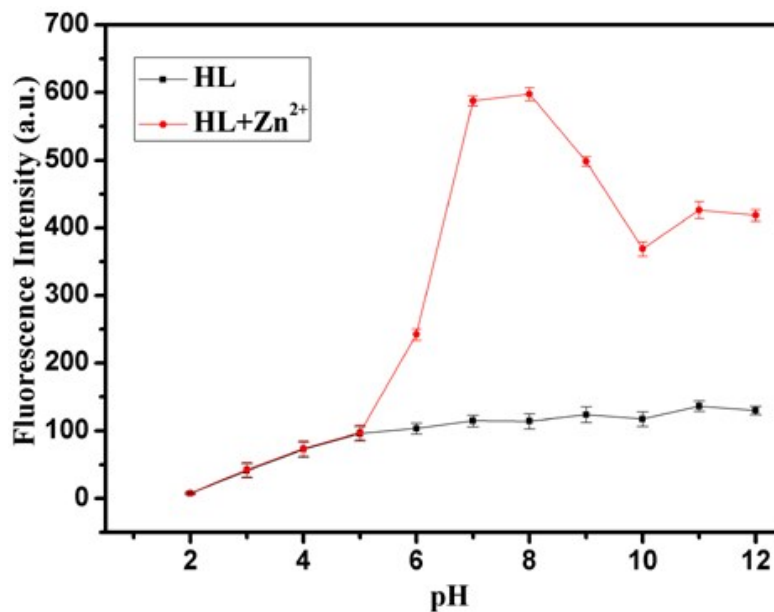
The pH test for HL with Zn^{2+} 

Figure S5. The pH influence on the fluorescence intensity of HL in the absence and presence of Zn^{2+} ion. Excitation wavelength: 330 nm. Error bars represent standard deviations from three repeated experiments.

UV-vis absorption of HL with Zn²⁺

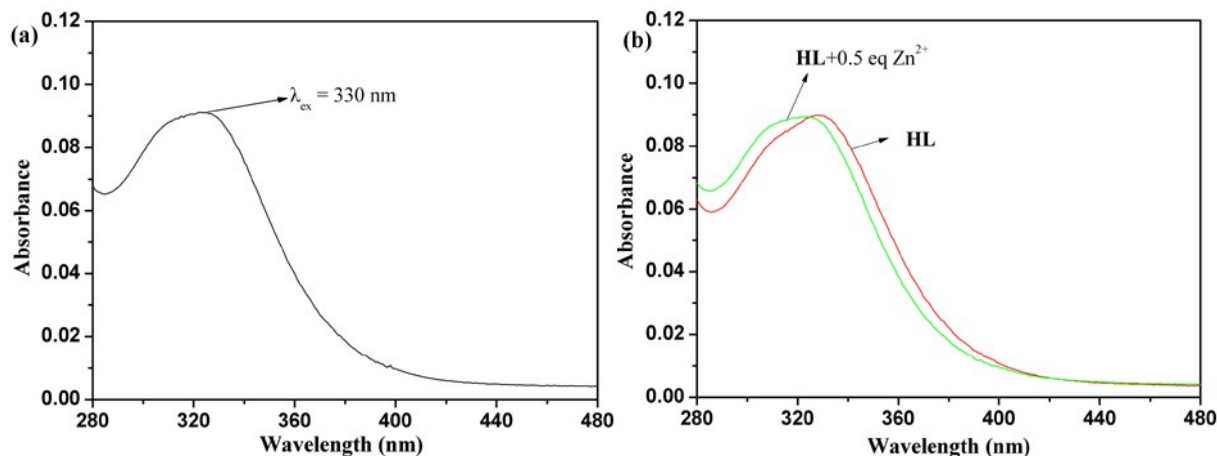


Figure S6. UV-vis spectra of HL (20 μM) (a) and upon addition of Zn²⁺ (0.5 equiv) (b) in 10 mM HEPES buffer solution at pH 7.4.

The binding constant of L-Zn

The association constant for 2:1 complex was calculated based on the titration curve of the chemosensors with metal ions. Association constants were determined by a nonlinear least squares fitting of the data with the following equation as referenced elsewhere.

$$y = \frac{x}{2 \times a \times b \times (1-x)^2} + \frac{x \times b}{2}$$

Where x is $(I-I_0)/(I_{\max}-I_0)$, y is the concentration of metal ions, a is the association constant, and b is the concentration of chemosensor.^{S1}

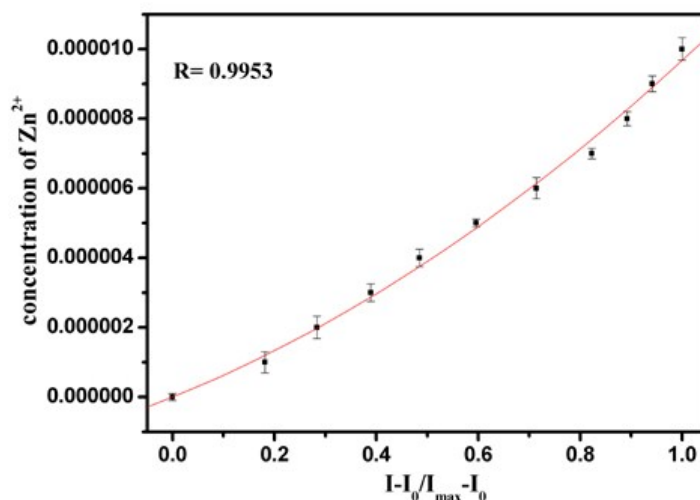


Figure S7. Fitting of fluorescence titration curve of HL with Zn²⁺ in 10 mM HEPES buffer at pH 7.4. Excitation wavelength: 330 nm. The binding constant of L-Zn is $8.75 \times 10^{10} \text{ M}^{-2}$. Error bars represent standard deviations from three repeated experiments.

The detection limit for Zn^{2+}

The limit of detection (LOD) was calculated based on the fluorescence titration. The emission intensity of **HL** without Zn^{2+} was measured 10 times, and the standard deviation of the blank measurements was determined. A good linear relationship between the fluorescence intensity at 545 nm and the Zn^{2+} concentrations could be obtained in the 0–1.50 μM concentration range ($R = 0.9985$). The limit of detection was then calculated as $\text{LOD} = 3\sigma/k$, where σ is the standard deviation of the blank measurements, and k is the slope of the intensity versus sample concentration.^{S2}

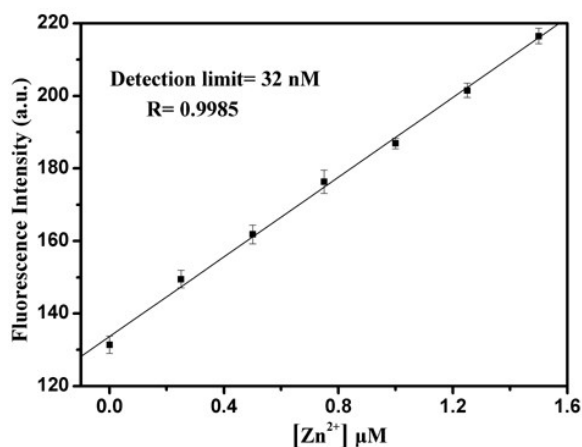


Figure S8. Fluorescence intensity at 545 nm for **HL** (20 μM) in aqueous solution (10 mM HEPES buffer, pH 7.4) as a function of the concentration of Zn^{2+} ($\lambda_{\text{ex}} = 330$ nm). The lowest detection limits of Zn^{2+} is 32 nM. Error bars represent standard deviations from five repeated experiments.

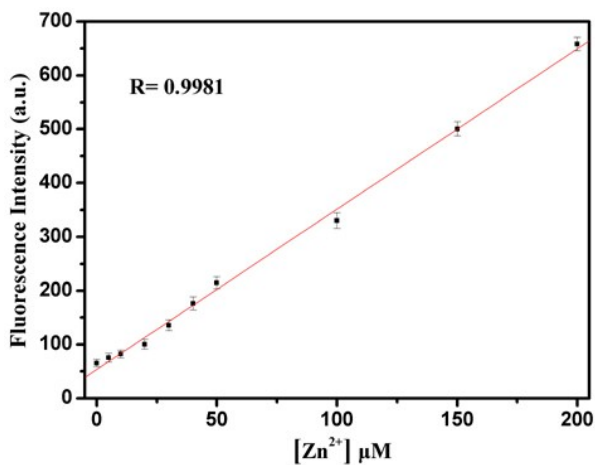
The intensity change of high concentration range

Figure S9. Fluorescence intensity at 545 nm for **HL** (400 μM) in aqueous solution (10 mM HEPES buffer, pH 7.4) as a function of the concentration of Zn^{2+} ($\lambda_{\text{ex}} = 330$ nm). The Zn^{2+} concentrations could be obtained in the 0–200 μM concentration range ($R = 0.9981$). Error bars represent standard deviations from three repeated experiments.

Fluorescence decay profile of HL, L-Zn

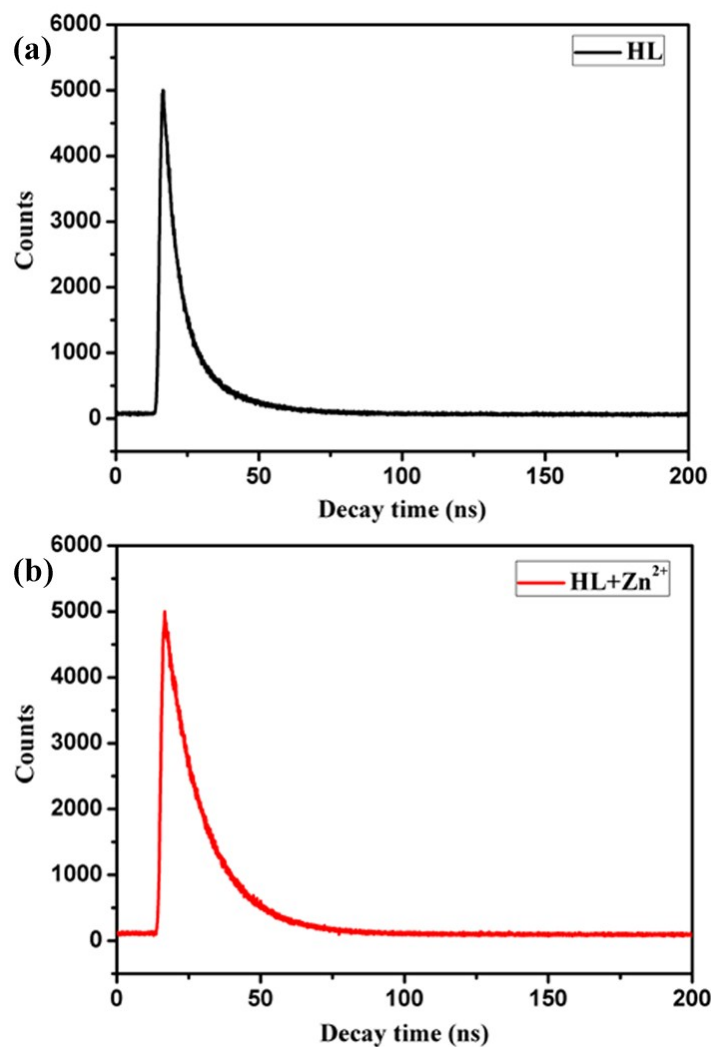


Figure S10. Fluorescence decay curve of **HL** (a), **L-Zn** (b). The lifetime of **HL** is 7.19 ns and contains two lifetime components: 4.61 ns (46.40%) and 9.44 ns (53.60%) (330 nm excitation, decay time at 545 nm emission). The lifetime of **L-Zn** is 14.64 ns (330 nm excitation, decay

time at 545 nm emission). The average lifetime was calculated according to $\langle \tau \rangle = \frac{\sum A_i \tau_i^2}{\sum A_i \tau_i}$.

The full range of mass spectrum of L-Zn

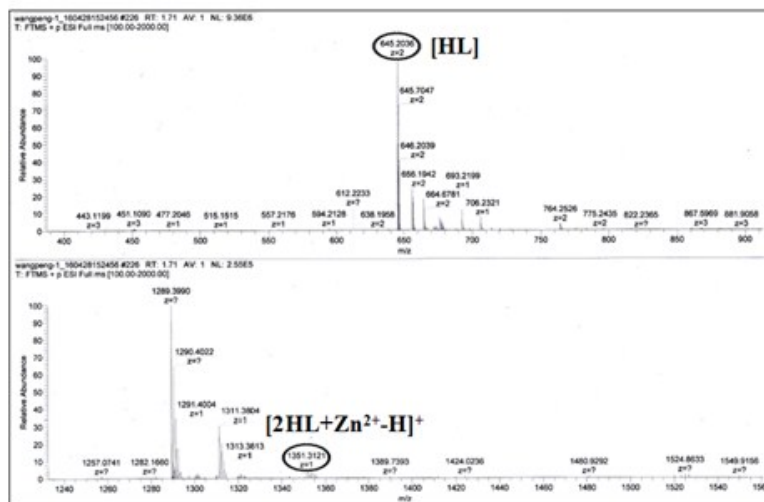


Figure S11. The full ESI mass spectrum of **HL** (500 μM) in $\text{H}_2\text{O}/\text{CH}_3\text{CN}$ (80/20, V/V, pH 7.4) including $\text{Zn}(\text{ClO}_4)_2$ (0.5 equiv).

The mass spectrum analysis of L-Zn

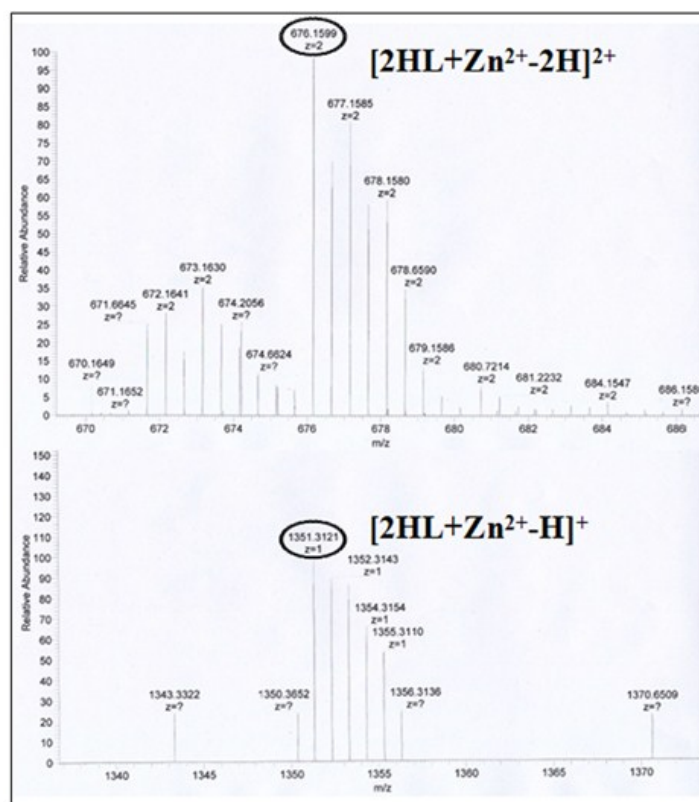


Figure S12. ESI mass spectrum of **HL** (500 μM) in $\text{H}_2\text{O}/\text{CH}_3\text{CN}$ (80/20, V/V, pH 7.4) including $\text{Zn}(\text{ClO}_4)_2$ (0.5 equiv).

The theoretical isotope patterns mass spectrum of L-Zn

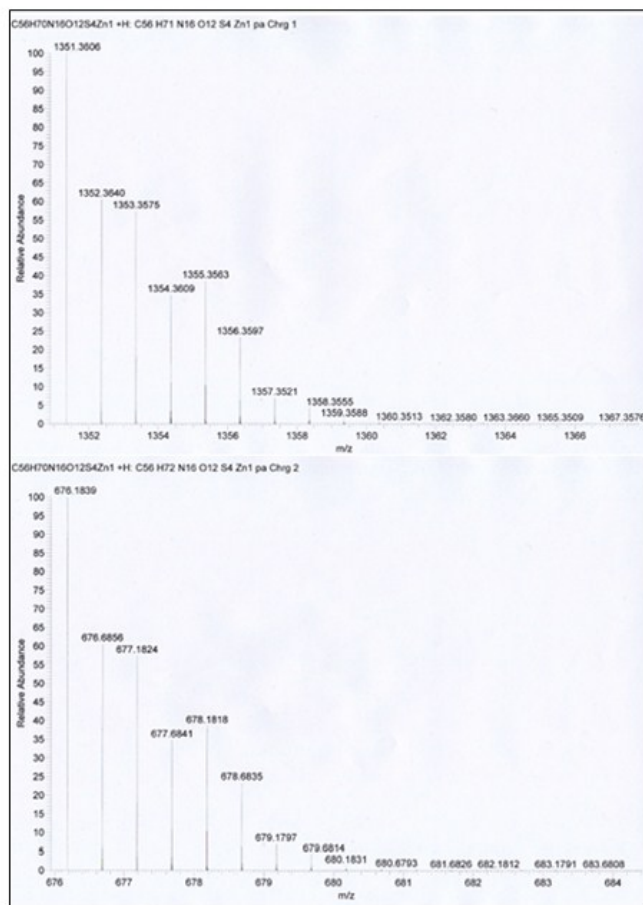


Figure S13. The theoretical isotope patterns mass spectrum of L-Zn.

Fluorescence response of L-Zn with EDTA

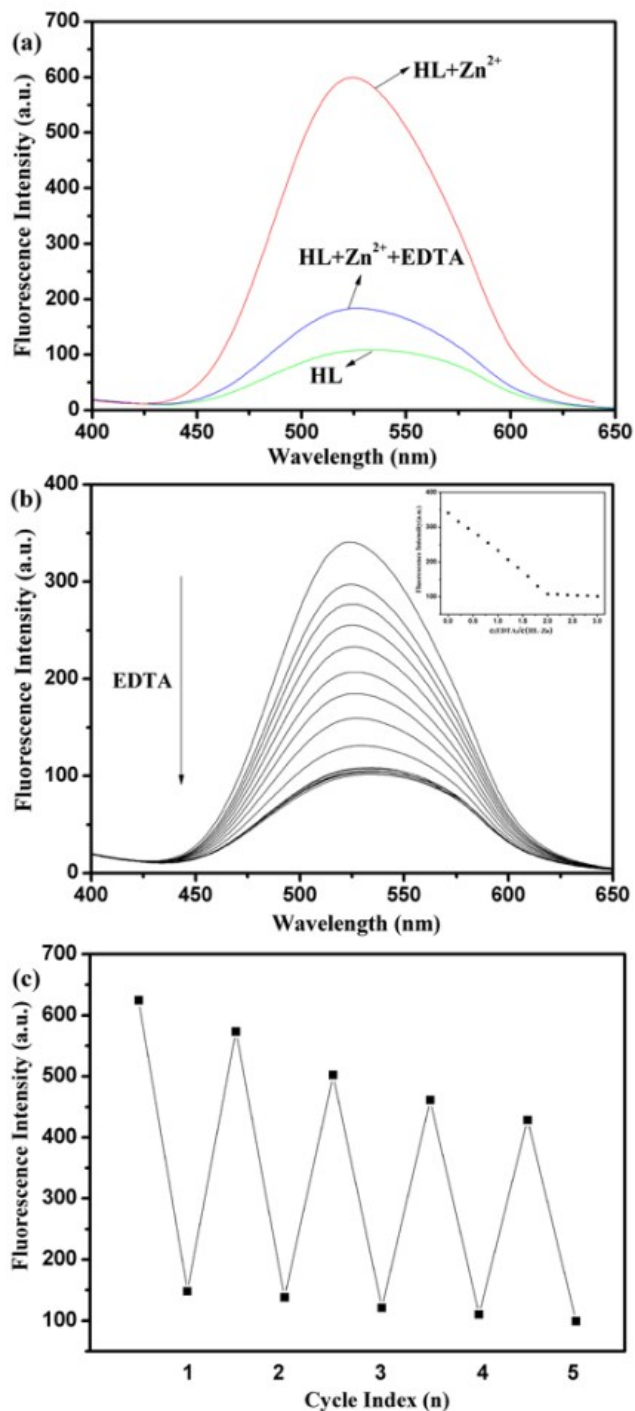


Figure S14. (a) Fluorescence emission spectra of L-Zn (10 μM) in the presence of EDTA in 10 mM HEPES buffer solution at pH 7.4. The molar ratio of EDTA : L-Zn is 2:1.(b) Fluorescence emission spectra of HL (10 μM) following addition of Zn²⁺ (0–3.0 equiv.) in 10 mM HEPES buffer solution at pH 7.4. (c) The cycle effect experiment with EDTA to Zn²⁺. Excitation wavelength: 330 nm.

Table S2. Compared with HL and the atomic absorption spectroscopy

Standard	Atomic Absorption Spectrometry Method	Peptide Chemosensor (HL)
----------	---------------------------------------	--------------------------

Solution	1	2	average	1	2	average
80 μM	5.4 mg/L(83.8 μM)	5.34 mg/L(82.2 μM)	5.395mg/L(83 μM)	78.3 μM	78.6 μM	78.5 μM
40 μM	2.48 mg/L(38.2 μM)	2.46 mg/L(37.8 μM)	2.47mg/L(38 μM)	39.1 μM	39.7 μM	39.4 μM

The optimized configurations for the ligand HL and complex L-Zn

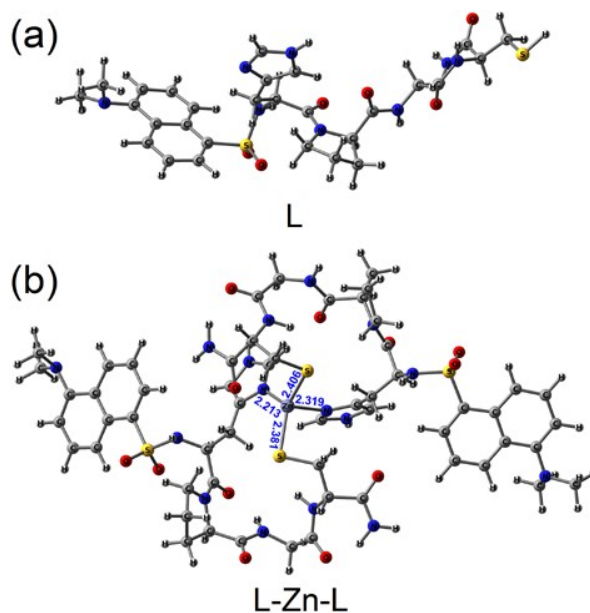


Figure S15. The optimized configurations for the ligand HL (a) and complex L-Zn (b).

The HOMO-LUMO energy gaps of HL and L-Zn

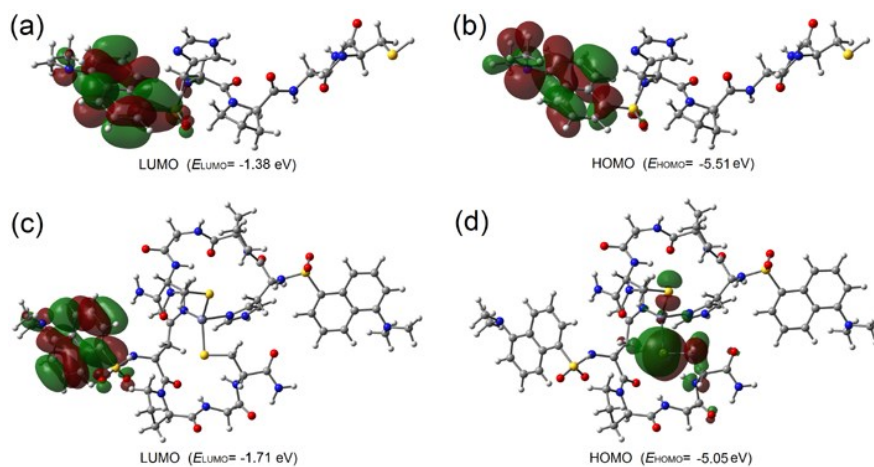


Figure S16. The HOMO-LUMO energy gaps for the respective compounds and the interfacial plots of the orbitals:(a) HL LUMO, (b) HL HOMO, (c) L-Zn LUMO, (d) L-Zn HOMO. The HOMO–LUMO energy gaps of HL is 4.13 eV and L–Zn is 3.34 eV.

Photo-induced electron transfer (PET) verification

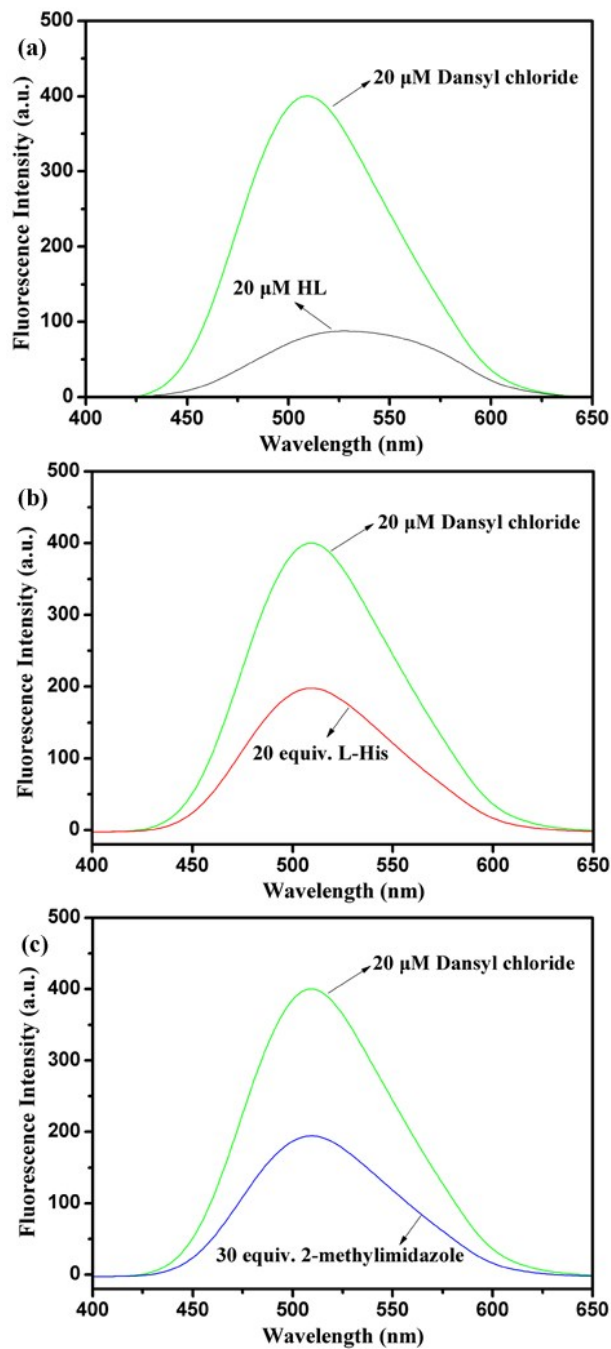
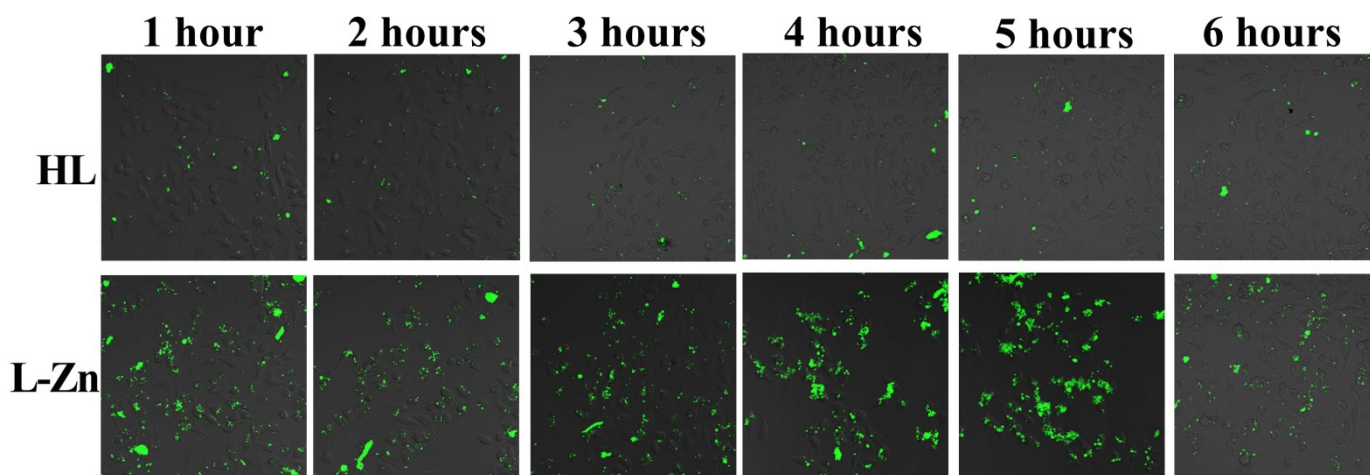


Figure S17. Fluorescence emission spectra of 20 μM dansyl chloride solution and 20 μM HL (a), and fluorescence emission spectra of 20 μM dansyl chloride solution following addition of 20 eq. L-His solution (b) and 30 eq. 2-methylimidazole (c) in 10 mM HEPES buffer solution at pH 7.4.

Table S3. The concentrations of Zn²⁺ and Cu²⁺ in live cells

Metal Ions	Concentration in Live Cells		
	1	2	average
Zn ²⁺	0.36 mg/L(5.54 μM)	0.37 mg/L(5.69 μM)	0.365 mg/L(5.62 μM)
Cu ²⁺	0.05 mg/L(0.78 μM)	0.03 mg/L(0.46 μM)	0.04 mg/L(0.62 μM)

The stability experiment of the HL in live cells**Figure S18.** Confocal fluorescence stability images of **HL** in HeLa cells: Merged transmission images of HeLa cells after incubation with 10 μM **HL**(top), 10 μM **HL** and 10 μM Zn²⁺ (bottom) at 37°C for 1-6 hours.

Fluorescence imaging of EDTA in live cells

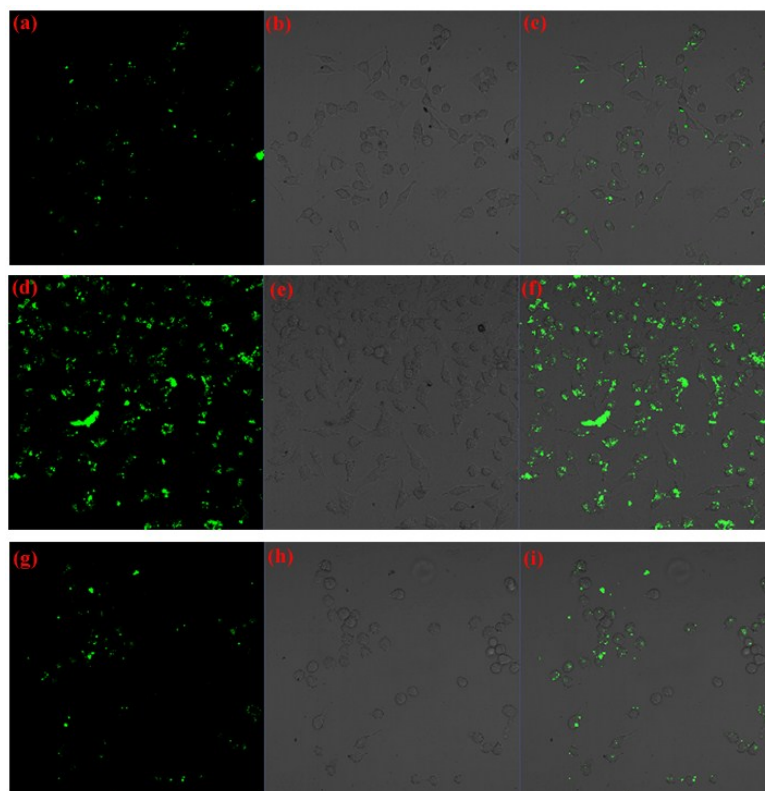


Figure S19. Confocal fluorescence images of HeLa cells: Fluorescence transmission images of HeLa cells after incubation with (a) 10 μM HL, (d) 10 μM HL and 10 μM Zn^{2+} , (g) 10 μM L-Zn and 20 μM EDTA for 30 min at 37°C. Bright-field transmission images (b, e, h,) and Merged transmission images (c, f, i,) of HeLa cells corresponding to part bright-field transmission images of HeLa cells (a, d, g, j), respectively.

Table S4. Comparison of chemosensors for Zn²⁺ assays in the literatures

Zn ²⁺ Chemosensor	Detection condition	Detection limit	Detection method	Reference
Schiff base derivative	Water	2.5 μ M	Turn-on	Org. Lett., 2012, 14 , 1214-1217
Mesoporous silica material	Aqueous solution	65 μ M	Turn-on	Adv. Funct. Mater., 2009, 19 , 223-234
Coumarin derivative	CH ₃ CN/H ₂ O(1:1 V/V)	65 μ M	Turn-on	RSC. Adv., 2014, 4 , 25341-25347
Quindine-Carbon dots	Aqueous solution	6.4 nM	Turn-on	J. Mater. Chem. B, 2014, 2 , 5020-5027
Hydroxyindole-Bodipy	CH ₃ CN	0.97 μ M	Ratiometric	Chem. Commun., 2012, 48 , 9897-9899
1,8-naphthalimide derivative	HEPES buffer	57 nM	Turn-on	Chem. Commun., 2013, 49 , 11430-11432
Two-photon	CH ₃ CN/H ₂ O(1:1 V/V)	10 μ M	Ratiometric	Chem. Sci., 2014, 5 , 3469-3474
2-methylquinoline	CH ₃ CN/H ₂ O(1:9 V/V)	198 nM	Turn-on	Sensors and Actuators B, 2013, 176 , 775-781
8-aminoquinoline	CH ₃ CN	1.85 μ M	Turn-on	Dalton Trans., 2014, 43 , 1881-1887
Luminescent-Iridium	Tris buffer	36 nM	Ratiometric	ACS. Appl. Mater. Interfaces., 2014, 6 , 14008-14015
Peptide	HEPES buffer	57 nM	Turn-on	This work

Reference

S1. L. N. Neupane, J. Y. Park, J. H. Park and K. H. Lee, *Org. Lett.* 2013, **15**, 254-257.

S2. L. N. Wang, W. W. Qin, X. L. Tang, W. Dou, W. S. Liu, Q. Teng, X. J. Yao, *Org. Bio. Chem.* 2010, **8**, 3751-3757.